OBSERVATIONS OF EXTENSIVE AIR SHOWERS BY AIR FLUORESCENCE SENSITIVITY TESTS AND RESULTS

G. L. Cassiday, H. E. Bergeson, T.-W. Chiu, D. A. Cooper, J. W. Elbert
E. C. Loh, D. Steck and W. J. West
Department of Physics, University of Utah
Salt Lake City, Utah 84112, U.S.A.

G. W. Mason
Department of Physics, Brigham Young University
Provo, Utah 84602, U.S.A.

J. Boone
Department of Physics, California Polytechnic State University
San Luis Obispo, California 93401, U.S.A.

J. Linsley
Department of Physics, University of New Mexico
Albuquerque, New Mexico 87131, U.S.A.

We present here experimental evidence that extensive air showers (EAS) have been detected via their isotropic light emission. In some cases, the light emitted from the shower was detected at emission angles up to 150° and at distances more than several Km away from the detector. Furthermore, on the basis of observed data rates and shower size determinations we demonstrate that the resultant sensitivity of the detector for observing EAS is consistent with expectations.

1. Introduction. Night sky radiation provides a flux of background light against which faint optical sources (such as EAS generated air fluorescence) must be detected. The relatively severe brightness of the night sky (about 10^6 photons sr^{-1} m^{-2} μsec^{-1} at Volcano Ranch, N.M.) coupled with the rather meager efficiency of the atmosphere as a scintillator (about 0.05%) might lead one to believe that an EAS would have to be improbably large in order to generate sufficient light to be visible to an optical detector. This requirement of large shower size coupled with a rapidly falling cosmic ray spectrum would thus render ineffectual almost any conceivable air fluorescence detection scheme. Thus, the fact that previous attempts at seeing EAS via the air fluorescence technique[1,2,3] have not achieved hoped-for results is easily explained. However, we present here overwhelming evidence that EAS can and, indeed, have been unambiguously detected via their isotropic optical emission and in the accompanying papers[4,5] we present additional evidence that on the basis of such optical measurements (1) shower sizes can be accurately determined, (2) experimentally viable event rates can be achieved for showers in the energy range $10^{16} < E < 10^{21}$ eV, and (3) the potentiality exists for measuring shower sizes throughout a reasonable portion of their trajectories, thus making possible a new class of EAS experiments.

2. EAS Source Strength and Triggering Sensitivity. Here we estimate how large an EAS must be in order to be seen by the Fly's Eye along with an assessment of the probability of simultaneous detection by the Fly's Eye and the Volcano Ranch Array. Shown in Fig. 6 (about which more will be said later) is

a reconstruction of one of the events actually seen simultaneously by the Fly's Eye and the Volcano Ranch Array. As a shower passes through the field of view $\Delta\theta$ of one of the photomultiplier "eyes," it will generate a photoelectron yield N_{pe}:

$$N_{pe} = N_e Y \frac{\varepsilon A}{4\pi R^2} \exp^{-R/\lambda} \Delta\ell \qquad (1)$$

where N_e = shower size in electrons
Y = fluorescent light yield (≈4 photons per meter per electron)
ε = combined light collection and photoelectron conversion efficiency (0.17 ± 20%)
A = effective light gathering area for mirror array ($1.7\ m^2$ ± 1%)
λ = attenuation length of 3600 Å photons in air (≈18 Km)
R = distance of EAS source from Fly's Eye
$\Delta\ell$ = differential path length along trajectory during which EAS is within field of view $\Delta\theta$

Letting θ be the optical emission angle for light seen by the Fly's Eye and $R\perp$ be the shower's impact parameter we have

$$\Delta\ell = \Delta(R\perp/\tan\theta) = R\perp\Delta\theta/\sin^2\theta \qquad (2)$$

Consequently, the size N_e of the EAS is

$$N_e \cong \frac{4\pi}{Y}\frac{1}{\varepsilon A}\frac{R\perp}{\Delta\theta} N_{pe} \qquad (3)$$

where we have neglected the attenuation of light due to atmospheric scattering since $R << \lambda$. Clearly, the accuracy which we can obtain in measuring N_e depends upon how accurately we can determine the factors $R\perp$ and N_{pe} for each event as well as the other factors which are essentially event independent. We might anticipate that scatter in our size measurements most certainly will result from inaccuracies in measuring $R\perp$ and N_{pe} from event to event. In particular N_{pe} is difficult to measure near threshold where noise and pulse slewing effects are most severe. We anticipate inaccuracies for near-threshold events of the order of ±(25-50)%. Systematic difficulties could result from uncertainties in the light generation yield factor Y. These effects will be more fully discussed in the following paper.

In order to trigger the Fly's Eye signal discriminators, the photoelectron current must induce a voltage pulse greater than some threshold value which is determined primarily by the night sky background. With our optics, each eye was bathed in enough light to generate about 6200 photoelectrons/μsec. The 1σ fluctuation in this number which represents the noise is about $80\sqrt{\tau}$ photoelectrons where τ is the pulse width. The voltage, then, at the input to the discriminators due to noise pulses of Nσ standard deviations is roughly

$$V \cong eG \frac{N_{pe}}{2\tau} R_o \left(1-e^{-\tau/T}\right) \qquad (4)$$

where e is the electron charge, G ($\cong 8\cdot10^6$) is the electronic gain of the detectors, R_o (≅75Ω) is the relevant input impedance, and T (=0.2 μsec) is the input filter time constant. Since noise photoelectrons scale as $\tau^{1/2}$ we obtain

$$V \simeq 40\ mV \frac{N}{\tau^{1/2}} \left(1-e^{-\tau/T}\right) \qquad (5)$$

where τ is in μsec and N is the number of standard deviations. We plot V vs τ in Fig. 1 for various values of N. Also shown by the solid line is the operating threshold ($V_T \approx 180$ mV) for our slow channel discriminators. (We ignore the fast channel which was primarily used for timing purposes.) In this experiment the range of impact parameters is about $0.75 \leq R \leq 2.25$ Km while the range of angles θ (see Fig. 6) is about ($20° \leq \theta \leq 150°$). These factors combine to yield a range of pulse widths (discussed in section 3) of about 100 nsec $\leq \tau \leq 1.3$ μsec. From the plot we estimate that all 5σ pulses regardless of pulse width should trigger the Fly's Eye.

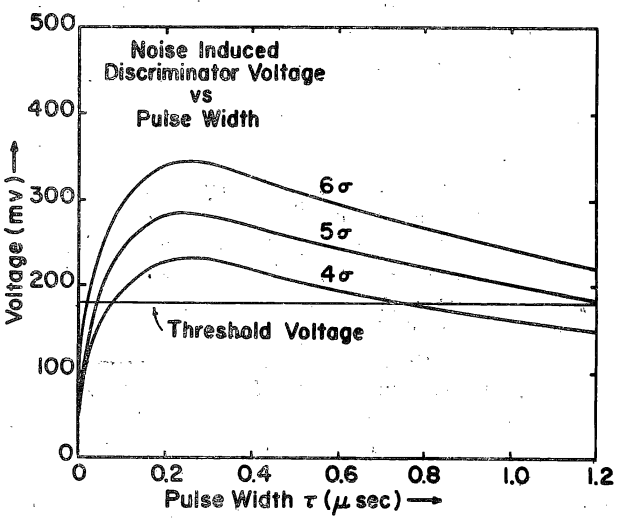

Fig. 1. Noise-induced discriminator voltage vs pulse width

We might note that our discriminator thresholds were under computer control throughout the course of the experiment. Count rates were monitored continuously from each photomultiplier and the discriminators adjusted up and down accordingly as the night sky brightness changed in order to preserve those counting rates. Single tube counting rates were thus fixed at about 100/sec thus holding the dead time constant to a value less than 1%. As a result of this count rate monitoring and control process, the relationship of the discriminator threshold to noise pulse size indicated in Fig. 1 was preserved. Hence, our triggering sensitivity was always as good as it could be for any given level of night sky brightness.

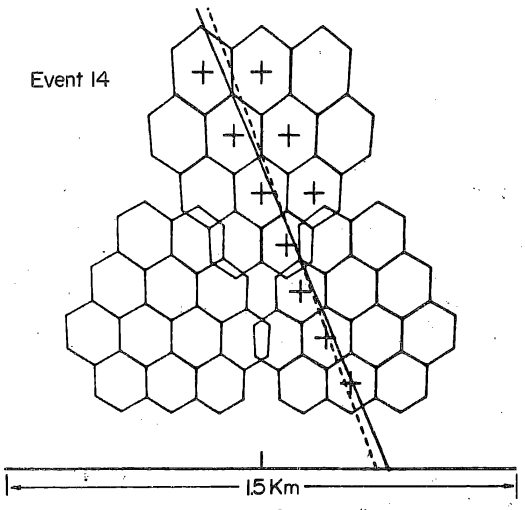

Fig. 2. Projection of EAS #14 as seen by the Fly's Eye onto a vertical plane above the Volcano Ranch Array. The solid line is the trajectory as determined by the Fly's Eye while the dotted line represents that determined by the VRA. The projected angles differ by 3°.

The actual triggering of the Fly's Eye event by event is a fairly complicated function of geometry, but we can roughly estimate from equation (3) and Fig.1 a minimum shower size necessary for a trigger. Let $R_\perp$ be 1 Km, then N_{pe} (5σ) is about 250 photoelectrons and from equation (3) we obtain N_e (threshold) $\approx 3.5 \cdot 10^7$ electrons. Due to electronic pulse slewing and our consequent inability to accurately measure pulse integrals for voltage levels near triggering threshold, we might expect an effective threshold

of $N_e \sim 5 \cdot 10^7$ electrons. This is a very fortuitous situation since VRA triggers on showers of such sizes about 1 per hour. Hence, a rate of 1 reasonably well-defined shower once every several hours of operation time is not an unreasonable expectation. These estimates are, in fact, close to reality since we detected 44 events in coincidence with VRA in about 100 hours running time during November 1976. The smallest of these events triggered only two photomultiplier eyes (the minimum number required for an "event" trigger) and typically the corresponding shower sizes were about $5 \cdot 10^7$ electrons.

3. Event Geometry. The crucial parameter of interest in the experiment is, of course, the number of shower electrons N_e as a function of its trajectory. In order to measure this number the trajectory first must be accurately determined. This can be done by locating the plane in space which contains the shower axis and then by locating the shower's impact parameter $R_\perp$ and its ground impact angle ψ (see Fig. 6). The Fly's Eye observables used to make these determinations are the geometrical pattern of the phototubes which were triggered by the shower along with their sequential timing which measured the progress of the shower through the Fly's Eye field of view. The geometrical triggering pattern is a direct measure of the shower's vertically projected zenith angle. This locates the shower-detector plane in space. We illustrate this by example for one of our observed events. Shown in Fig. 2 is a projection of the 3 Fly's Eye mirror clusters onto the vertical plane above the center of the VRA. The horizontal extent of the VRA is about 1.5 Km and unfortunately we do not completely cover its field of view. To some extent we

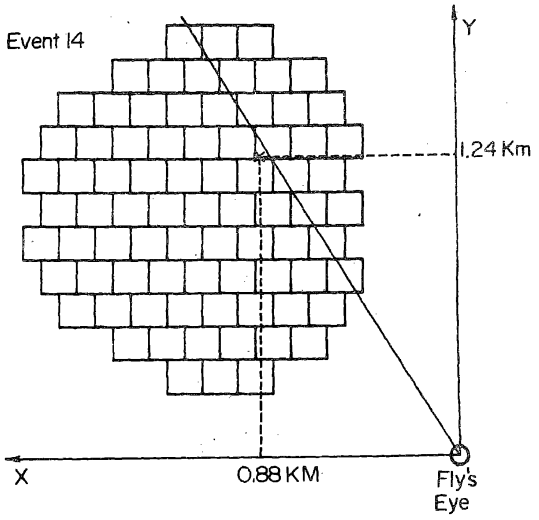

Fig. 3. Projection of the plane containing the axis of EAS #14 and the Fly's Eye (the shower-detector plane) onto the horizontal VRA. The core location of the shower as determined by the VRA is denoted by X.

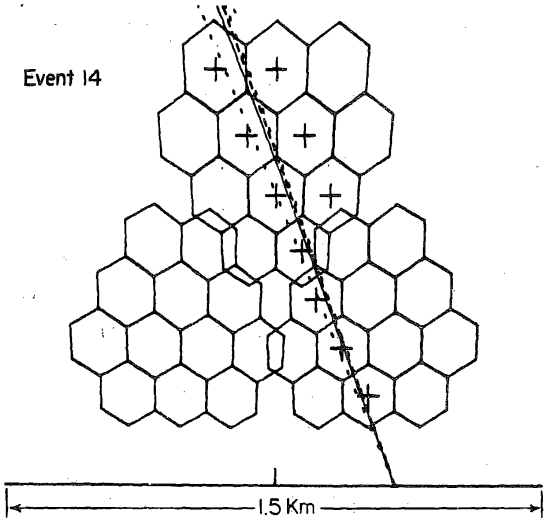

Fig. 4. Fit to the vertical projection of EAS #14 as seen by the Fly's Eye obtained by constraining the ground impact point to the position determined by the VRA. The projected angle determined by the VRA and the Fly's Eye is nearly identical.

sacrificed total coverage (and subsequent event rate) by positioning the field of view of mirror 1 above mirrors 2 and 3 in order to gain more redundant information on a select sample of events. The X's in that figure indicate those "eyes" which were triggered by shower #14. Note that the shower makes a fairly well-defined line through our field of view. Furthermore, each eye was triggered in a well-defined time sequence, progressing downwards along the X's.

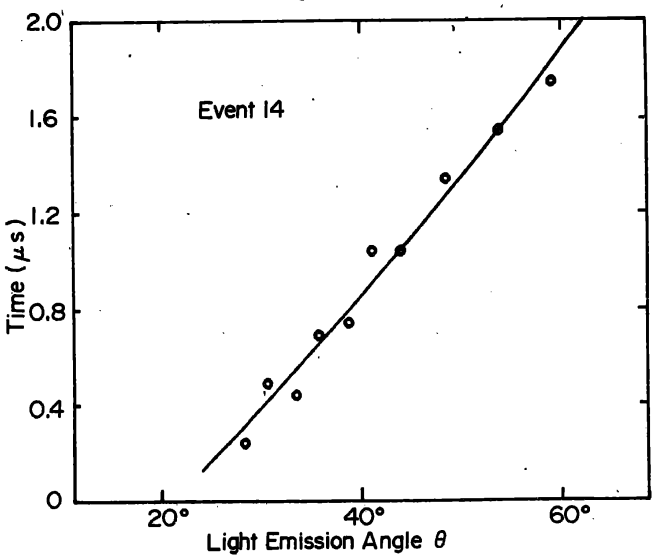

Fig. 5. Time in μsec at which a given photomultiplier "eye" in the Fly's Eye (indicated by the X's in Fig. 2 and 4) triggered on the light generated by EAS #14 as it passed through the field of view.

Shown in Fig. 3 is a horizontal view of VRA. The projection of the shower-detector plane onto this horizontal plane is indicated by the straight line extending from the Fly's Eye. This particular shower impacted the ground 1.52 Km away as determined by the VRA and marked by the X. In order to determine $R_\perp$ and ψ from our timing data we constrain the shower to impact the ground at this position. The result of this constraint is pictured in Fig. 4. We now show in Fig. 5 a plot of the elapsed time of the shower as it passes through the field of view of each eye. The actual values of these elapsed times can be used to determine $R_\perp$ and ψ (see Fig. 6) in the following way: since the shower travels at the same speed as the light it generates, the light reaching the Fly's Eye lags the passing shower front by a time

$$t(\theta)=\frac{R_\perp}{c\sin\theta}-\frac{R_\perp}{c\tan\theta}=\frac{R_\perp}{c}\tan\frac{\theta}{2}$$

(Eq. 6). A best fit of the data to this timing function yields the shower axis indicated by the solid line in Fig. 6.

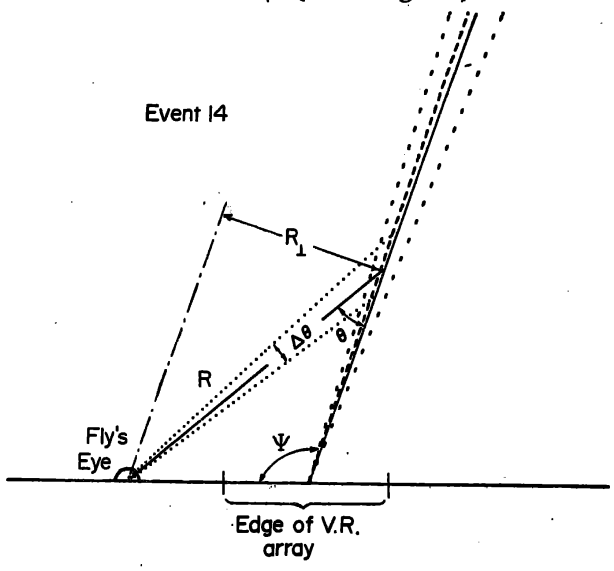

Fig. 6. The solid line indicates the geometrical reconstruction of the shower trajectory using the Fly's Eye spatial and timing data. The dashed line represents the VRA-determined trajectory.

4. Results. We present in Table 1 the results of our geometrical analysis for each of the 16 events (out of a total of 44) for which we had a maximum "2 mirror" field of view. In all cases, agreement with VRA-determined parameters is quite good. The average value for our projected zenith

Table 1

Comparison of EAS Geometry as Determined by Fly's Eye and VRA

	Projected Zenith Angle ϕ						Ground-Impact Angle ψ			Net Space-Angle Difference
	Unconstrained			Constrained			Constrained			
Event #	Utah	VRA	$\Delta\phi$	Utah	VRA	$\Delta\phi$	Utah	VRA	$\Delta\psi$	$\Delta\beta$
2	-21	- 6	15	-17	- 6	11	108	113	5	11
4	-19	-36	17	-25	-36	11	122	120	2	9
13	-11	-13	2	-13	-13	0	62	46	16	17
14	-23	-20	3	-20	-20	0	111	109	2	1
17	- 2	- 5	3	- 8	- 5	3	87	78	9	10
18	4	9	5	10	9	1	111	106	5	5
25	- 1	-14	13	- 8	-14	6	118	127	9	11
26	17	20	3	25	20	5	58	69	11	12
28	-28	-32	4	-21	-32	11	98	115	17	20
29	- 6	6	12	0	6	6	108	90	18	19
31	-22	-19	3	-20	-19	1	85	91	6	6
32	38	28	10	30	28	2	112	117	5	6
37	5	10	5	13	10	3	123	121	2	4
39	10	- 3	13	1	- 3	4	95	97	2	5
42	35	17	18	27	17	10	105	126	21	24
44	18	5	13	7	5	2	84	76	8	9
Averages			8.7°	-1.2°	-3.3°	4.8°	99°	100°	8.6°	10.6°

angle is -1.2°, thus no systematic geometrical bias is indicated. Events enter and leave our field of view from each direction with equal probability. The average ground impact angle $\bar{\psi}$ (99°) indicates a mild bias for events coming somewhat towards the Fly's Eye. This is to be expected due to the enhancement of triggering probability at small angles θ via directly beamed or forward-scattered Cherenkov light. Nonetheless, it is extremely unlikely that such light could result in significant triggering enhancement at angles $\theta \gtrsim 45°$. This effect will be discussed in the next paper.

We conclude by reasserting our conviction that EAS have been unambiguously detected at distances far from our detector via their isotropic optical emissions.

Acknowledgements This work is supported by the National Science Foundation, Washington, D.C., U.S.A.

References

1. Greisen, K. 1965, Proc. 9th Int. Conf. on Cosmic Rays (London), p. 609.
2. Chudakov, A. 1962, 5th Inter-American Seminar on Cosmic Rays (Bolivia).
3. Tanahashi, G. et al. 1975, Proc. 14th Int. Conf. on Cosmic Rays (Munich) 12, p. 4385-4390.
4. Mason, G.W. et al. 1977, accompanying paper in these proceedings.
5. Elbert, J.W. et al. 1977, accompanying paper in these proceedings.